embodies the details of the fragmentation mechanism and the assumptions and simplifications concerning magma rheology and degassing. As $\eta$ and $\dot{\gamma}$ are predicted to increase very rapidly in a narrow conduit region in response to magma degassing (Fig. 1), relatively large variations in the value of $X$ do not lead to significant displacements of the calculated fragmentation level, and the two mechanisms show good agreement in the predicted fragmentation conditions.

The model reported here makes predictions that are in line with experiments and observations, as follows: the consistency between the experimental conditions for brittle magma fragmentation and the fluid dynamics of magma ascent; the calculated range of gas volume fraction at fragmentation in close agreement with measured pumice vesicularities; the inverse relationship between pumice vesicularity and magma viscosity (which is observed in natural samples and suggested by the modelling results); and the discrimination between high-viscosity (mainly explosive) and low-viscosity (mainly effusive) eruptions. This suggests that the proposed criterion for magma fragmentation could be operating during sustained explosive eruptions. □

Received 2 March; accepted 9 October 1998.


1. Dingwell, D. B. Volcanic dilemma: flow or blow? *Science* **273,** 1054–1055 (1996).
2. Mader, H. M. *et al*. Experimental simulations of explosive degassing of magma. *Nature* **372,** 85–88 (1994).
3. Phillips, J. C., Lane, S. J., Lejeune, A. M. & Hilton, M. The gum rosin-acetone system as an analogue to the degassing behaviour of hydrated magmas. *Bull. Volcanol.* **57,** 263–268 (1995).
4. Mader, H. M., Phillips, J. C., Sparks, R. S. J. & Sturtevant, B. Dynamics of explosive degassing of magma: observations of fragmenting two-phase flows. *J. Geophys. Res.* **101,** 5547–5560 (1996).
5. Alidivirov, M. & Dingwell, D. B. Magma fragmentation by rapid decompression. *Nature* **380,** 146–148 (1996).
6. Zimanowski, R. B., Büttner, R., Lorentz, V. & Häfele, H. G. Fragmentation of basaltic melt in the course of explosive volcanism. *J. Geophys. Res.* **102,** 803–814 (1997).
7. Zhang, Y., Sturtevant, B. & Stolper, E. M. Dynamics of gas-driven eruptions: experimental simulations using $CO_2$-$H_2O$-polymer system. *J. Geophys. Res.* **102,** 3077–3096 (1997).
8. Wohletz, K. H., Sheridan, M. F. & Brown, W. K. Particle size distributions and sequential fragmentation\transport theory applied to volcanic ash. *J. Geophys. Res.* **94,** 15703–15721 (1989).
9. Alidivirov, M. A. A model for viscous magma fragmentation during volcanic blasts. *Bull. Volcanol.* **56,** 459–465 (1994).
10. Barmin, A. A. & Mel'nik, O. É. Eruption dynamics of high-viscosity gas-saturated magmas. *Izv. Ros. Akad. Nauk. Mekh. Zhidk. Gaza* **2,** 49–60 (1993).
11. Wilson, L., Sparks, R. S. J. & Walker, G. P. L. Explosive volcanic eruptions–IV. The control of magma properties and conduit geometry on eruption column behaviour. *Geophys. J. R. Astron. Soc.* **63,** 117–148 (1980).
12. Dobran, F. Nonequilibrium flow in volcanic conduits and application to the eruptions of Mt. St. Helens on May 18, 1980, and Vesuvius in AD 79. *J. Volcanol. Geotherm. Res.* **49,** 285–311 (1992).
13. Papale, P. Dobran, F. Modeling of the ascent of magma during the plinian eruption of Vesuvius in AD 79. *J. Volcanol. Geotherm. Res.* **58,** 101–132 (1993).
14. Papel, P. Dobran, F. Magma flow along the volcanic conduit during the Plinian and pyroclastic flow phases of the May 18, 1980, Mount St. Helens eruption. *J. Geophys. Res.* **99,** 4355–4373 (1994).
15. Ramos, J. I. One-dimensional, time-dependent, homogeneous, two-phase flow in volcanic conduits. *Int. J. Num. Methods Fluids* **21,** 253–278 (1995).
16. Woods, A. W. & Bower, S. M. The decompresison of volcanic jets in a crater during explosive volcanic eruptions. *Earth Planet. Sci. Lett.* **131,** 189–205 (1995).
17. Papale, P. From magma to tephra: Modeling physical processes of explosive volcanic eruptions (eds Freundt, A. & Rosi, M.) *Developments in Volcanology* (Elsevier, Amsterdam, in the press).
18. Dingwell, D. B. & Webb, S. L. Structural relaxation in silicate melts and non-Newtonian melt rheology in geologic processes. *Phys. Chem. Miner.* **16,** 508–516 (1989).
19. Webb, S. L. & Dingwell, D. B. Non-Newtonian rheology of igneous melts at high stresses and strain rates: experimental results for rhyolite, andesite, basalt, and nephelinite. *J. Geophys. Res.* **95,** 15695–15701 (1990).
20. Dingwell, D. B. The brittle-ductile transition in high-level granitic magmas: material constraints. *J. Petrol.* **38,** 1635–1644 (1997).
21. Thomas, N., Jaupart, C. & Vergniolle, S. On the vesicularity of pumice. *J. Geophys. Res.* **99,** 15633–15644 (1994).
22. Maxwell, J. C. On the dynamical theory of gases. *Phil. Trans. R. Soc. Lond.* **157,** 49–88 (1867).
23. Sparks, R. S. J. The dynamics of bubble formation and growth in magmas: a review and analysis. *J. Volcanol. Geotherm. Res.* **3,** 1–37 (1978).
24. Lejeune, A.-M. & Richet, P. Rheology of crystal-bearing silicate melts: an experimental study at high viscosities. *J. Geophys. Res.* **100,** 4215–4229 (1995).
25. Mangan, M. T. & Cashman, K. V. The structure of basaltic scoria and reticulite and inferences for vesiculation, foam formation, and fragmentation in lava fountains. *J. Volcanol. Geotherm. Res.* **73,** 1–18 (1996).
26. Whitham, A. G. & Sparks, R. S. J. Pumice. *Bull. Volcanol.* **48,** 209–223 (1986).
27. Houghton, B. F. & Wilson, C. J. N. A vesicularity index for pyroclastic deposits. *Bull. Volcanol.* **51,** 451–462 (1989).
28. Klug, C. & Cashman, K. V. Permeability development in vesiculating magmas: implications for fragmentation. *Bull. Volcanol.* **58,** 87–100 (1996).
29. Kaminsky, E. & Jaupart, C. Expansion and quenching of vesicular magma fragments in Plinian eruptions. *J. Geophys. Res.* **102,** 12187–12203 (1997).


**Acknowledgements.** This work was supported by the Italian Gruppo Nazionale per la Vulcanologia, and performed when the author was a member of the Volcanic Simulation Group of Pisa.

Correspondence and requests for materials should be addressed to the author (e-mail: papale@dst.unipi.it).

# A neuronal representation of the location of nearby sounds

**Michael S. A. Graziano, Lina A. J. Reiss & Charles G. Gross**

*Department of Psychology, Princeton University, Princeton, New Jersey 08544, USA*

**Humans can accurately perceive the location of a sound source—not only the direction, but also the distance[1–9]. Sounds near the head, within ducking or reaching distance, have a special saliency. However, little is known about this perception of auditory distance. The direction to a sound source can be determined by interaural differences, and the mechanisms of direction perception have been studied intensively[1]; but except for studies on echolocation in the bat[10], little is known about how neurons encode information on auditory distance. Here we describe neurons in the brain of macaque monkeys (*Macaca fascicularis*) that represent the auditory space surrounding the head, within roughly 30 cm. These neurons, which are located in the ventral premotor cortex, have spatial receptive fields that extend a limited distance outward from the head.**

The ventral premotor cortex (PMv) is a multimodal, sensorymotor area located in the frontal lobe just anterior to primary motor cortex. Most PMv neurons respond to touch, and about 40% also respond to visual stimuli[11–16]. For these bimodal neurons, the visual receptive field extends from the region of the tactile receptive field into the space immediately adjacent (Fig. 1a). These neurons usually do not respond to distant visual stimuli, more than 30 cm from the tactile receptive field. That is, they represent the space near the body, within the monkey's reach. Here we studied neurons in PMv whose tactile receptive fields included the back of the monkey's head, and found that 53% were trimodal, responding to tactile, visual and auditory stimuli (Table 1). The mean auditory response latency was 46 ms (s.d. = 10.9 ms).

Figure 1b shows the responses of a typical trimodal neuron. The tactile receptive field (stippled) covered the contralateral side of the head. The neuron responded to visual stimuli within about 20 cm of the contralateral side of the face. In addition to these tactile and visual responses, the neuron also responded to sounds produced near the contralateral side of the head. Jingling keys, claps, crinkling paper, and bursts of white noise all gave strong responses. Sine waves of various frequencies (200–3,200 Hz) did not elicit responses. To test the auditory receptive field, six speakers were arranged around the head at the azimuth angles shown (Fig. 1b) and at a distance of 10 cm, and bursts of white noise were presented for 0.3 s. The neuron responded to all six speaker positions, but preferred position 2, near the contralateral side of the face (Fig. 1b). That is, the auditory receptive field matched the location of the visual and tactile receptive fields, although the tactile receptive field was larger and also included the back of the head. The calculated preferred direction of the auditory response for this neuron was 27° contralateral to the direction that the monkey was facing.

Figure 1c shows the results for 43 trimodal neurons. Each arrow

**Table 1 Number of neurons in the different response categories**

| | Tactile response on back of head | No tactile response on back of head |
|---|---|---|
| Unresponsive | – | 70 |
| Visual | – | 12 |
| Auditory | – | 1 |
| Tactile | 10 | 51 |
| Tactile + visual | 67 | 64 |
| Tactile + visual + auditory | 88 | 3 |
| Total | 165 | 201 |

represents the preferred auditory direction for one neuron. The auditory responses in PMv clearly span the entire contralateral space, and seem to represent the space in front of the head (31 neurons) more densely than the space behind the head (12 neurons; $\chi^2 = 8.4$, $P < 0.01$). Almost all neurons with an auditory response also responded to a touch on the ears or back of the head (Table 1). Yet the tactile receptive fields of these trimodal neurons were rarely restricted to the back of the head (9/91, 10%); most also included parts of the cheek, eyebrow, snout or jaw (82/91, 90%). Likewise, the visual receptive fields were sometimes located in the periphery and sometimes extended into the centre of the visual field. That is, the trimodal neurons in PMv do not form a back-of-the-head representation, but instead form a complete representation of the space around the head. As already described, the visual representation in PMv emphasizes the space within reaching distance. Do the auditory receptive fields have a similar spatial limit?

Figure 2 shows data from four trimodal neurons. We manipulated both the amplitude of the sound and the distance between the speaker and the head. In Fig. 2a, the neuron responded to sounds presented 10 cm from the head. Sounds presented 30 or 50 cm away did not elicit a response, even though they covered the same range of amplitudes measured at the head. The effect of distance on the response of the neuron was statistically significant, but there was no significant overall effect of the amplitude of the sound on the response of the neuron (see regression analysis in legend of Fig. 2). Data from another neuron are shown in Fig. 2b. Like the cell in Fig. 2a, this neuron responded significantly better to closer stimuli, but unlike that cell, it responded significantly better to higher-amplitude stimuli as well. The neuron in Fig. 2c had an inhibitory response to auditory stimuli and an excitatory response to tactile stimuli. It responded best, that is, had the lowest firing rate, to sounds presented 10 cm away, and responded less well to sounds at 30 or 50 cm. Again the effect both of distance and of amplitude was significant. We often found trimodal neurons with an inhibitory auditory response and an excitatory tactile response, or vice versa (17 of 91 trimodal neurons, 19%). This result demonstrates that the response to nearby sounds is not caused by the sound mechanically stimulating the tactile receptive field. Finally, for the neuron in Fig. 2d, the response showed no significant dependence on the distance to the sound source, and instead depended on the amplitude of the sound.

In total, 44 neurons (34 in monkey 1, 10 in monkey 2) were tested for dependence on stimulus amplitude and distance. Of these, 15

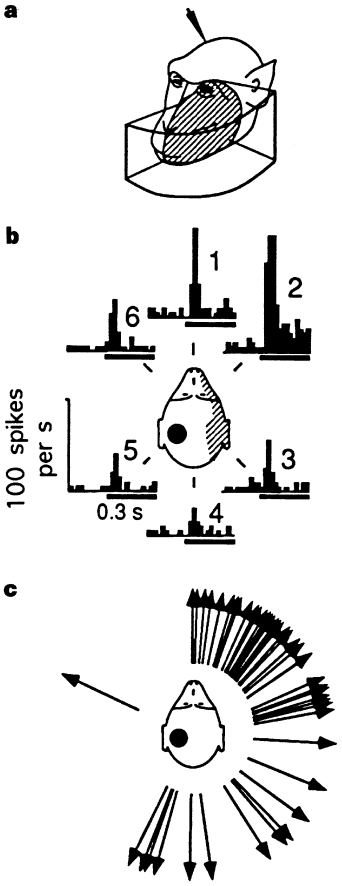


**Figure 1** Responses of bimodal and trimodal neurons in PMv. **a**, Receptive fields of a typical bimodal, visual-tactile neuron. The tactile receptive field (shaded) is on the front of the face contralateral to the recording electrode (indicated by the arrowhead). The visual receptive field (boxed) is confined to a region of space within about 10 cm of the tactile receptive field. **b**, Responses of a typical trimodal, visual–tactile–auditory neuron. The tactile receptive field is contralateral to the recording electrode (indicated by the black spot) and includes the ear and back of the head. The visual receptive field (not shown) extends about 20 cm into the space near the contralateral side of the face. The histograms show the response, summed over ten trials, to a burst of white noise presented 10 cm away at the indicated azimuth angles. **c**, The calculated preferred direction of the auditory response for 43 trimodal neurons. Each arrow shows the result for one neuron. Preferred direction is given by $(\Sigma\phi_n r_n)/\Sigma r_n$, where $\phi_n$ = the angular position of speaker $n$, and $r_n$ = the neuron's response to speaker $n$ (mean number of spikes per s in the stimulus period).

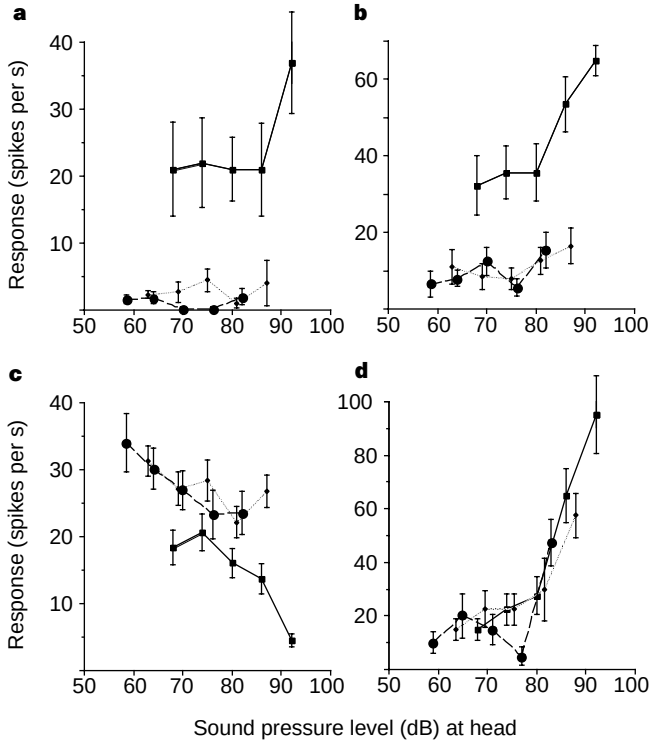


**Figure 2** Auditory responses of four trimodal neurons to white noise, presented at five amplitudes and three distances from the head. *x*-axis, sound pressure level of stimulus measured at the head; *y*-axis, response of neuron in spikes per s. Distance of speaker from the head: squares, 10 cm; diamonds, 30 cm; circles, 50 cm. Each point is based on ten trials. Error bars, standard error of the mean. The neurons in **a** and **b** responded best to the closest stimuli. The neuron in **c** had an inhibitory response; it responded better (lower firing rate) to closer stimuli. In **d**, the neuron responded better to higher-amplitude stimuli, but showed no sensitivity to the distance of the stimulus. A linear regression analysis[26] was done to test the significance of the effect of distance ($t_d$) and of amplitude ($t_a$) independently of each other. For the neuron in **a**, $t_d = -7.194$, $P < 0.001$; $t_a = 1.335$, $P = 0.184$; **b**, $t_d = -7.235$, $P < 0.001$; $t_a = 3.711$, $P < 0.001$; **c**, $t_d = 4.225$, $P < 0.001$; $t_a = -4.745$, $P < 0.001$; **d**, $t_d = -1.241$, $P = 0.217$; $t_a = 7.549$, $P < 0.001$.

(34%) responded significantly better to closer stimuli but were unaffected by the amplitude of the stimulus; 15 (34%) responded significantly better to higher-amplitude stimuli but were unaffected by the distance to the stimulus; and 11 (25%) responded significantly better to closer stimuli and, independently, to higher-amplitude stimuli. Amplitude is one of many possible cues that humans use to determine the distance to an auditory event[17]. Therefore, we suggest that the amplitude-sensitive neurons described here use this particular cue to code distance. These neurons will tend to respond to nearby stimuli because they respond better to higher-amplitude sounds. However, more than half of the neurons (59%) code distance by means of some other cue or combination of cues, such that they respond to nearby stimuli independently of the amplitude. Reverberation of the sound from the walls of the room may be important[18]. Another possible set of cues for distance involves familiarity with the sound source[19]. However, the first neuron tested in monkey 2 was significantly dependent on distance even though the monkey had never heard the stimulus before. Another possible cue is the difference in amplitude between the two ears; a very large difference implies a sound source close to one ear. However, the neurons were sensitive to distance even when the stimulus was presented on the midline, that is, when the amplitude was equal in both ears. Finally, the calculation of distance near the head may depend on the highly complex distorting effect of the head and pinnae on the sound spectrum[1]. This last effect would be especially pronounced at such close distances as 10 cm. A full analysis of the relative influence of these different cues will require further experiments.

The cortical pathways for auditory spatial processing are not well understood. Perhaps distance information is calculated in a different brain area and then relayed to the trimodal neurons in PMv. Recently, we studied neurons in a portion of parietal area 7b[20], in the upper bank of the later sulcus, and found similar trimodal, tactile–visual–auditory neurons (M.S.A.G. and C.G.G., manuscript in preparation). Area 7b projects to PMv[21,22], but whether the trimodal region of 7b projects to the trimodal region of PMv has not yet been determined.

Previous experiments showed that multimodal neurons in PMv encode the locations of nearby objects, within about reaching distance, through touch, vision, and even visual memory[11–16]. Our results show that PMv neurons also represent nearby auditory space. Because a high proportion of PMv neurons respond during movements of the head, mouth, arms and hands, the purpose of this multimodal map of space may be to guide movements towards and around the objects that surround the body[23,24]. □

### Methods

Two adult *M. fascicularis* were trained to sit in a primate chair; they did not perform any task. (For details of the experimental procedures, see ref. 16.) During daily recording sessions, a microdrive was used to lower an electrode into PMv. Once a neuron was isolated, it was tested for somatosensory, visual and auditory responses. Somatosensory receptive fields were plotted by manipulating the joints and stroking the skin. Visual receptive fields were plotted with objects presented on a wand. Auditory stimuli included tones, clicks, claps, jingling keys and other sounds. Controlled tests were done using white noise (20–22,000 Hz) presented over Cambridge Soundworks 3-inch (76.2 mm) speakers mounted in a circular array around the monkey's head at ear level. The angular position and distance of the speakers to the head was adjustable. The sound pressure level of the stimuli was measured at the monkey's head using a Radio Shack sound level meter, repeatedly calibrated with a 0.25-inch (6.35 mm) Bruel and Kjaer microphone. Neurons were tested either with the speaker behind the head, or in the dark, so that the monkey could not see the distance to the sound source. Eye position was not controlled during the presentation of auditory stimuli. Some PMv neurons are influenced by eye position[14,16,25]. However, the short latency of the auditory response eliminates the possibility that it was caused by a change in eye position elicited by the presentation of the stimulus. In addition, there are no reports of transient bursts of activity in PMv associated with eye movement, whereas most of the auditory responses in PMv were transient, short-latency bursts (Fig. 1b).

Received 29 September; accepted 23 November 1998.


1. Blauert, J. *Spatial Hearing: The Psychophysics of Human Sound Localization* (transl. Allen, J. S.) (MIT Press, Cambridge, Massachusetts, 1997).
2. Clifton, R. K., Rochat, P., Robin, D. J. & Berthier, N. E. Multimodal perception in the control of infant reaching. *J. Exp. Psychol. Hum. Percept. Perform.* **20,** 876–886 (1994).
3. Coleman, P. D. An analysis of cues to auditory depth perception in free space. *Psychol. Bull.* **60,** 302–315 (1963).
4. Coleman, P. D. Dual role of frequency spectrum in determination of auditory distance. *J. Acoust. Soc. Am.* **44,** 631–632 (1968).
5. Edwards, A. A. Accuracy of auditory depth perception. *J. Gen. Psychol.* **52,** 327–329 (1955).
6. Gamble, E. A. Intensity as a criterion in estimating the distance of sounds. *Psychol. Rev.* **16,** 416–426 (1909).
7. Gardner, M. B. Distance estimation of 0° or apparent 0°-oriented speech signals in anechoic space. *J. Acoust. Soc. Am.* **45,** 47–53 (1969).
8. Mershon, D. H. & Bowers, J. N. Absolute and relative cues for the auditory perception of egocentric distance. *Perception* **8,** 311–322 (1979).
9. von Bekesy, G. *Experiments in Hearing* (McGraw-Hill, New York, 1960).
10. Suga, N. & O'Neill, W. E. Neural axis representing target range in the auditory cortex of the mustache bat. *Science* **206,** 351–353 (1979).
11. Gentilucci, M. *et al.* Functional organization of inferior area 6 in the macaque monkey. I. Somatotopy and the control of proximal movements. *Exp. Brain. Res.* **71,** 475–490 (1988).
12. Fogassi, L. *et al.* Coding of peripersonal space in inferior premotor cortex (area F4). *J. Neurophysiol.* **76,** 141–157 (1996).
13. Graziano, M. S. A., Yap, G. S. & Gross, C. G. Coding of visual space by pre-motor neurons. *Science* **266,** 1054–1057 (1994).
14. Graziano, M. S. A., Hu, X. & Gross, C. G. Coding the locations of objects in the dark. *Science* **277,** 239–241 (1997).
15. Rizzolatti, G. *et al.* Afferent properties of periarcuate neurons in macaque monkeys. II. Visual responses. *Behav. Brain Res.* **2,** 147–163 (1981).
16. Graziano, M. S. A., Hu, X. & Gross, C. G. Visuo-spatial properties of ventral premotor cortex. *J. Neurophysiol.* **77,** 2268–2292 (1997).
17. Ashmead, D. H., LeRoy, D. & Odom, R. D. Perception of the relative distances of nearby sound sources. *Percept. Psychophys.* **47,** 326–331 (1990).
18. Mershon, D. H. & King, L. E. Intensity and reverberation as factors in the auditory perception of egocentric distance. *Percept. Psychophys.* **18,** 409–415 (1975).
19. Coleman, P. D. Failure to localize the source distance of an unfamiliar sound. *J. Acoust. Soc. Am.* **34,** 345–346 (1962).
20. Graziano, M. S. A., Fernandez, T. & Gross, C. G. A comparison of bimodal, visual-tactile neurons in parietal area 7b and ventral premotor cortex of the monkey brain. *Neurosci. Abs.* **22,** 398 (1996).
21. Cavada, C. & Goldman-Rakic, P. S. Posterior parietal cortex in rhesus monkey: II: Evidence for segregated corticocortical networks linking sensory and limbic areas with the frontal lobe. *J. Comp. Neurol.* **287,** 422–445 (1989).
22. Matelli, M., Camarda, R., Glickstein, M. & Rizzolatti, G. Afferent and efferent projections of the inferior area 6 in the macaque monkey. *J. Comp. Neurol.* **255,** 281–298 (1986).
23. Graziano, M. S. A. & Gross, C. G. Spatial maps for the control of movement. *Curr. Opin. Neurobiol.* **8,** 195–201 (1998).
24. Rizzolatti, G., Fadiga, L., Fogassi, L. & Gallese, V. The space around us. *Science* **277,** 190–191 (1997).
25. Boussaoud, D., Barth, T. M. & Wise, S. P. Effects of gaze on apparent visual responses of frontal cortex neurons. *Exp. Brain Res.* **93,** 423–434 (1993).
26. Cohen, J. & P. Cohen, P. *Applied Multiple Regression/Correlation Analysis for the Behavioral Sciences* (Lawrence Earlbaum Associates, Hillsdale, New Jersey, 1983).


**Acknowledgements.** We thank E. Olson, X. Hu, S. Alisharan, M. E. Wheeler and V. Gomez for their help during the experiment.

Correspondence and requests for materials should be addressed to M.S.A.G. (e-mail: graziano@princeton.edu).

# Perception's shadow: long-distance synchronization of human brain activity

**Eugenio Rodriguez, Nathalie George, Jean-Philippe Lachaux, Jacques Martinerie, Bernard Renault & Francisco J. Varela**

*Laboratoire de Neurosciences Cognitives et Imagerie Cérébrale (LENA), CNRS UPR 640, Hôpital de la Salpétrière, 47 Boulevard de l'Hôpital, 75651 Paris Cedex 13, France*

**Transient periods of synchronization of oscillating neuronal discharges in the frequency range 30–80 Hz (gamma oscillations) have been proposed to act as an integrative mechanism that may bring a widely distributed set of neurons together into a coherent ensemble that underlies a cognitive act[1–4]. Results of several experiments in animals provide support for this idea (see, for example, refs 4–10). In humans, gamma oscillations have been**